

Steric Parameters of Conformationally Flexible Ligands from X-ray Structural Data. 1. P(OR)₃ Ligands in Equivalent Ligand Environments

Jeremy M. Smith, Neil J. Coville,* Leanne M. Cook, and Jan C. A. Boeyens

Department of Chemistry, University of the Witwatersrand, P.O. Wits 2050, South Africa

Received April 24, 2000

The complexes [Mo(η^5 -C₅H₅)(CO)₂(L)I] (L = P(OMe)₃, P(OEt)₃, P(OⁱPr)₃, P(OⁱBu)₃, P(OⁿPn)₃) were prepared and characterized by X-ray crystallography. Crystallographic cone (θ_C) and solid (Ω_C) angles for the phosphite ligands were calculated from the ligand conformations in the crystal structures and compared with the available literature data. The steric data are shown to be influenced by the surrounding ligand environment. The effects of the ligand conformation on the steric measurements are discussed, and the results applied to the analysis of equilibrium *cis*–*trans* isomer ratios in [Mo(η^5 -C₅H₅)(CO)₂(L)I].

Introduction

The quantification of ligand effects, particularly those of phosphorus(III) ligands,^{1–4} has been important in understanding and predicting the behavior of organometallic systems in terms of linear free energy relationships.^{5–15} The effects of various ligands on reacting systems are typically described in terms of steric and electronic properties, and a correlation is established between the molecular property under consideration and these stereoelectronic properties (eq 1).

$$\text{property} = a + b(\text{electronic}) + c(\text{steric}) \quad (1)$$

Other parameters, such as an "aryl effect",^{8,16} may also be included in this relationship. Clearly, for such quantitative descriptions of systems, reliable ligand parameters are required. The electronic parameters³ are usually described in terms of pK_a ^{7,11} or χ ^{11,17} values, and

various attempts have been made to separate out σ - and π -effects.^{7,11,18} Steric effects are usually described in terms of the Tolman cone angle, θ .^{1,19} However, in principle, other measures, such as solid angles, Ω ,^{4,20} and ligand repulsive energies, E_R ,^{2,21–23} may also be used. *The most important requirement for parameters to be used reliably is self-consistency and transferability among many systems.*

The Tolman cone angle, θ , is generally accepted as a reasonably reliable descriptor of ligand steric requirements.²⁴ Being a geometric measure, it is crucial that the cone angle is measured from a reasonable and realistic ligand conformation. In addition to the original methodology,^{1,19} cone angles measured from ligand conformations determined by *ab initio*²⁵ and molecular mechanics calculations²⁶ and X-ray crystallography^{27,28} and from crystal data in the Cambridge Structural Database (CSD)²⁹ have been found for the most part to compare favorably with the original θ values. However, in certain instances, the reported values of θ have been questioned, in particular for ligands that have multiple conformational possibilities. Thus, the cone angle values for some phosphite ligands, with flexible carbon chains, have been found from crystallographic and other structural analyses^{2–4,30,31} to be underestimated. This un-

- (1) Tolman, C. A. *Chem. Rev.* **1977**, *77*, 313–348.
- (2) Brown, T. L.; Lee, K. J. *Coord. Chem. Rev.* **1993**, *128*, 89–116.
- (3) Dias, P. B.; Piedade, M. E. M. d.; Simões, J. A. M. *Coord. Chem. Rev.* **1994**, *135/136*, 737–807.
- (4) White, D.; Coville, N. J. *Adv. Organomet. Chem.* **1994**, *36*, 95–158.
- (5) Bartholomew, J.; Fernandez, A. L.; Lorsche, B. A.; Wilson, M. R.; Prock, A.; Giering, W. P. *Organometallics* **1996**, *15*, 295–301.
- (6) Fernandez, A. L.; Lee, T. Y.; Reyes, C.; Prock, A.; Giering, W. P. *Organometallics* **1998**, *17*, 3169–3175.
- (7) Golovin, M. N.; Rahman, M. M.; Belmonte, J. E.; Giering, W. P. *Organometallics* **1985**, *4*, 1981–1991.
- (8) Wilson, M. R.; Woska, D. C.; Prock, A.; Giering, W. P. *Organometallics* **1993**, *12*, 1742–1752.
- (9) Eriks, K.; Giering, W. P.; Liu, H.-Y.; Prock, A. *Inorg. Chem.* **1989**, *28*, 1759–1763.
- (10) Rahman, M. M.; Liu, H. Y.; Prock, A.; Giering, W. P. *Organometallics* **1987**, *6*, 650–658.
- (11) Rahman, M. M.; Liu, H.-Y.; Eriks, K.; Prock, A.; Giering, W. P. *Organometallics* **1989**, *8*, 1–7.
- (12) Poë, A. J.; Farrar, D. H.; Zheng, Y. *J. Am. Chem. Soc.* **1992**, *114*, 5146–5152.
- (13) Moreno, C.; Macazaga, M. J.; Delgado, S. *Organometallics* **1991**, *10*, 1124–1130.
- (14) Haar, C. M.; Nolan, S. P.; Marshall, W. J.; Moloy, K. G.; Prock, A.; Giering, W. P. *Organometallics* **1999**, *18*, 474–479.
- (15) Farrar, D. H.; Poë, A. J. *J. Am. Chem. Soc.* **1994**, *116*, 6252–6261.
- (16) Farrar, D. H.; Hao, J.; Poë, A. J.; Stromnova, T. A. *Organometallics* **1997**, *16*, 2827–2832.

- (17) Bartik, T.; Himmler, T.; Schulte, H.-G.; Seevogel, K. *J. Organomet. Chem.* **1984**, *272*, 29–41.
- (18) Pacchioni, G.; Bagus, P. S. *Inorg. Chem.* **1992**, *31*, 4391–4398.
- (19) Tolman, C. A. *J. Am. Chem. Soc.* **1970**, *92*, 2956–2965.
- (20) White, D.; Taverner, B. C.; Leach, P. G. L.; Coville, N. J. *J. Comput. Chem.* **1993**, *36*, 1042.
- (21) Brown, T. L. *Inorg. Chem.* **1992**, *31*, 1286–1294.
- (22) Caffrey, M. L.; Brown, T. L. *Inorg. Chem.* **1991**, *30*, 3907–3914.
- (23) Choi, M.-G.; Brown, T. L. *Inorg. Chem.* **1993**, *32*, 5603–5610.
- (24) Boyles, M. L.; Brown, D. V.; Drake, D. A.; Hostetler, C. K.; Maves, C. K.; Mosbo, J. A. *Inorg. Chem.* **1985**, *24*, 3126–3131.
- (25) DeSanto, J. T.; Mosbo, J. A.; Storhoff, B. N.; Bock, P. L.; Bloss, R. E. *Inorg. Chem.* **1980**, *19*, 3086–3092.
- (26) Chin, M.; Durst, G. L.; Head, S. R.; Bock, P. L.; Mosbo, J. A. *J. Organomet. Chem.* **1994**, *470*, 73–85.
- (27) Clark, H. C.; Hampden-Smith, M. J. *Coord. Chem. Rev.* **1987**, *79*, 229–255.
- (28) Hughes, R. P.; Smith, J. M.; Liable-Sands, L. M.; Concolino, T. E.; Lam, K.-C.; Incarvito, C.; Rheingold, A. L. *J. Chem. Soc., Dalton Trans.* **2000**, 873–879.
- (29) Müller, T. E.; Mingos, D. M. P. *Transition Met. Chem.* **1995**, *20*, 533–539.

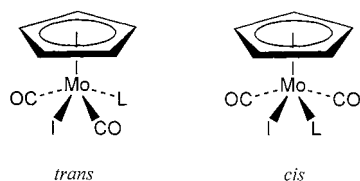


Figure 1. *Cis-trans* isomers for $[\text{Mo}(\eta^5\text{-C}_5\text{H}_5)(\text{CO})_2(\text{L})\text{I}]$ complexes.

derestimation has been further confirmed by studies of steric and electronic effects on atom transfer reactions of $\text{Re}(\text{CO})_4\text{L}^*$ radicals.³²

For flexible ligands, such as the alkyl phosphites, the conformation of a ligand, and hence its steric parameters, will be influenced by the other ligands around the metal (intramolecular forces), which determine the space, or ligand pocket, available for L. In the solid state, intermolecular forces may also play a role. We have thus deliberately chosen a single system, $[\text{Mo}(\eta^5\text{-C}_5\text{H}_5)(\text{CO})_2(\text{L})\text{I}]$, in which *only* the phosphite ligand is varied in order to keep the environment around the ligand reasonably constant. This approach contrasts with one entailing the evaluation of the ligand conformations of a large series of complexes, in *varying environments*.²⁹ For comparison with our data, we have determined steric parameters from another series of complexes in which only the phosphite ligand, L, is varied, $[\text{W}(\text{I})_2(\text{CO})_2(\text{L})(\text{Ph}_2\text{P}(\text{CH}_2)_2\text{PPh}_2)]$,³³ which may not necessarily have the same size ligand pocket.

In this paper, we have determined the steric parameters (crystallographic cone, θ_c , and solid, Ω_c , angles) of the alkyl phosphite ligands from their X-ray structural data in both series of molybdenum and tungsten complexes. Further, the molybdenum complexes exhibit *cis-trans* isomerism (Figure 1),³⁴ with the isomeric ratio dependent on both electronic and steric factors.³⁵ Thus by correlation of the equilibrium isomer ratio with the measured steric parameters we hope to test the applicability of our ligand steric values.

Results and Discussion

Synthesis and Characterization. Treating dichloromethane solutions of $[\text{Mo}(\eta^5\text{-C}_5\text{H}_5)(\text{CO})_3\text{I}]$ with the phosphite ligand, L, in the presence of Me_3NO ³⁶ gave the complexes $[\text{Mo}(\eta^5\text{-C}_5\text{H}_5)(\text{CO})_2(\text{L})\text{I}]$ (L = $\text{P}(\text{OMe})_3$,^{35,37} $\text{P}(\text{OEt})_3$, $\text{P}(\text{O}^i\text{Pr})_3$, $\text{P}(\text{O}^i\text{Bu})_3$, $\text{P}(\text{O}^n\text{Pn})_3$) **1–5**. The complexes were purified by column chromatography and crystallized from CH_2Cl_2 /hexanes mixtures as dark red crystals. All complexes were found to be air and thermally stable, with the exception of **4**, which slowly decomposed in the solid state at room temperature.

Table 1. K_{Eq} , the Equilibrium *Cis/Trans* Isomer Ratio for **1–5**

complex	L	$K_{\text{Eq}} = \text{cis:trans}$
1	$\text{P}(\text{OMe})_3$	0.11 ± 0.01
2	$\text{P}(\text{OEt})_3$	0.67 ± 0.07
3	$\text{P}(\text{O}^i\text{Pr})_3$	1.2 ± 0.10
4	$\text{P}(\text{O}^i\text{Bu})_3$	0.77 ± 0.08
5	$\text{P}(\text{O}^n\text{Pn})_3$	0.83 ± 0.08

All complexes were characterized by elemental analysis and IR and ^1H NMR spectroscopy. As with previous work,³⁵ we were unable to use the infrared spectra to assign the isomers of these complexes. However, we were able to assign isomers by ^1H NMR spectroscopy. The cyclopentadienyl ring protons of the *trans* isomer resonates as a phosphorus-coupled doublet in the ^1H NMR spectra, while those of the *cis* isomer produce a singlet at higher field.³⁵ Further confirmation was obtained from the resonances of the phosphite ligands, for which the lower symmetry of the *cis* isomer results in more complicated spectra.³⁵

On this basis, we found that all complexes crystallized exclusively as the *trans* isomer. The *cis* isomers were prepared and characterized by solution isomerization studies, for which K_{Eq} , the equilibrium *cis/trans* isomer ratio, is listed in Table 1. To probe the possibility of *trans*→*cis* isomerization occurring in the solid state,^{38–40} crystalline samples of the pure *trans* isomers were heated in a DSC apparatus. However, only endotherms corresponding to either the melting or decomposition of the isomer under study were observed.

X-ray Single-Crystal Study. The crystal structures of the complexes $[\text{Mo}(\eta^5\text{-C}_5\text{H}_5)(\text{CO})_2(\text{L})\text{I}]$ (L = $\text{P}(\text{OEt})_3$, $\text{P}(\text{O}^i\text{Pr})_3$, $\text{P}(\text{O}^i\text{Bu})_3$, $\text{P}(\text{O}^n\text{Pn})_3$) **2–5** were determined by single-crystal X-ray crystallography at room temperature. The structure of **1** has been previously reported.³⁷ Two independent molecules were detected in the unit cell of **2**. In complex **5** the methyl groups of the phosphite ligand were found to be disordered over three positions, while the iodide ligand was disordered over five positions. Complex **4** was found to decompose during the data collection, and the data obtained were not considered to be of good enough quality to permit further crystallographic discussion ($R1 = 0.0565$, $wR2 = 0.1447$). However, we were able to determine the connectivity of the complex and found this information sufficient to determine steric parameters for the ligand (see below). The refined structures together with the atomic-numbering scheme are shown in Figures 2–5. Selected bond lengths and angles of **2**, **3**, and **5** are listed in Table 1. The respective data for **1** are also listed.

As expected, all of the complexes adopt a square pyramidal “piano-stool” structure. The bond lengths and angles around the molybdenum atom do not show any unusual deviations from previously reported distances,⁴¹ and thus the different phosphite ligands appear to have a negligible effect on the geometry around the metal atom. Thus, the space available to the ligands, the ligand pocket, will be similar in all complexes, and the

(30) Stahl, L.; Ernst, R. D. *J. Am. Chem. Soc.* **1987**, *109*, 5673–5680.

(31) Stahl, L.; Trakarnpruk, W.; Freeman, J. W.; Arif, A. M.; Ernst, R. D. *Inorg. Chem.* **1995**, *34*, 1810–1814.

(32) Hanckel, J. M.; Lee, K.-W.; Rushman, P.; Brown, T. L. *Inorg. Chem.* **1986**, *25*, 1852–1856.

(33) Baker, P. K.; Drew, M. G. B.; Johans, A. W.; Haas, U.; Latif, L. A.; Meecham, M. M.; Zanin, S. *J. Organomet. Chem.* **1999**, *590*, 77–87.

(34) King, R. B. *Inorg. Chem.* **1963**, *2*, 936–944.

(35) Faller, J. W.; Anderson, A. S. *J. Am. Chem. Soc.* **1970**, *92*, 5852–5860.

(36) Blumer, D. J.; Barnett, K. W.; Brown, T. L. *J. Organomet. Chem.* **1979**, *173*, 71–76.

(37) Hardy, A. D. U.; Sim, G. A. *J. Chem. Soc., Dalton Trans.* **1972**, 1900.

(38) Beach, D. L.; Dattilo, M.; Barnett, K. W. *J. Organomet. Chem.* **1977**, *140*, 47–51.

(39) Cheng, L.; Coville, N. J. *Organometallics* **1996**, *15*, 867–871.

(40) Filippou, A. C.; Winter, J. G.; Feist, M.; Kociok-Köhn, G.; Hinz, I. *Polyhedron* **1998**, *17*, 1103–1114.

(41) Orpen, A. G.; Brammer, L.; Allen, F. H.; Kennard, O.; Watson, D. G.; Taylor, R. *J. Chem. Soc., Dalton Trans.* **1989**, S1–S83.

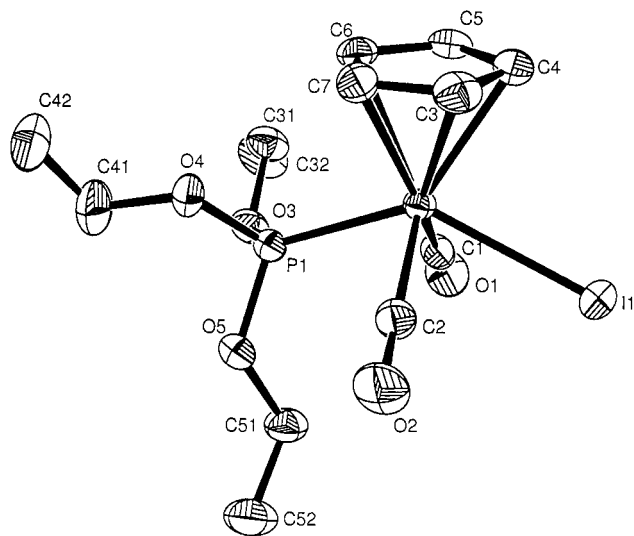


Figure 2. ORTEP diagram and atomic numbering scheme of one of the two independent molecules of $[\text{Mo}(\eta^5\text{-C}_5\text{H}_5)(\text{CO})_2(\text{P}(\text{OEt})_3)\text{I}]$, **2**. Hydrogen atoms omitted for clarity. Thermal ellipsoids shown at 30% probability.

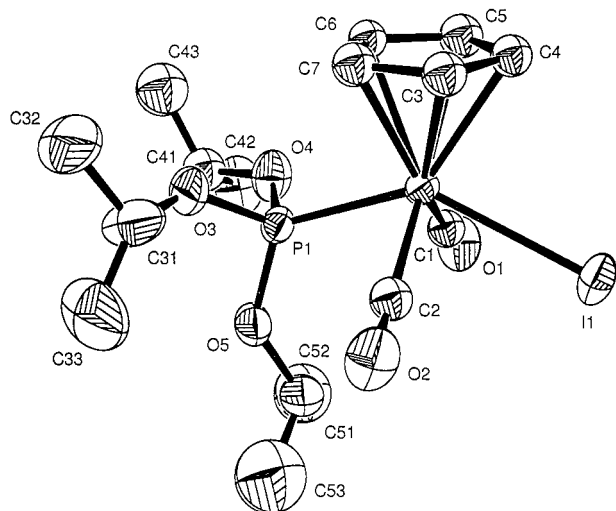


Figure 3. ORTEP diagram and atomic numbering scheme of $[\text{Mo}(\eta^5\text{-C}_5\text{H}_5)(\text{CO})_2(\text{P}(\text{O}^i\text{Pr})_3)\text{I}]$, **3**. Hydrogen atoms omitted for clarity. Thermal ellipsoids shown at 30% probability.

arrangement of the ligand atoms close to the metal should be similar for all ligands. In this region of space the P–O bond lengths are all similar and do not show any unusual deviations from literature values,⁴¹ while the Mo–P–O bond angles always show the same relative arrangement. The Mo–P(1)–O(4) bond angle, which corresponds to the phosphite arm which is bent away from the metal, is always smaller, and closer to 109.5°, than the Mo–P–O bond angles of the other two arms, which are all within 3° of each other. This suggests that the ligand pocket prevents the other two arms, which are bent back toward the metal, from achieving ideal values. Further, the cen–Mo(1)–P(1)–O(5) torsion angles (Table 2) reveal that the rotational orientation of the phosphite ligands relative to the cyclopentadienyl ring is remarkably similar in all complexes, although some variability in the exact orientation is observed.

Further away from the metal, where the ligand atoms are less constrained by the ligand pocket, there is

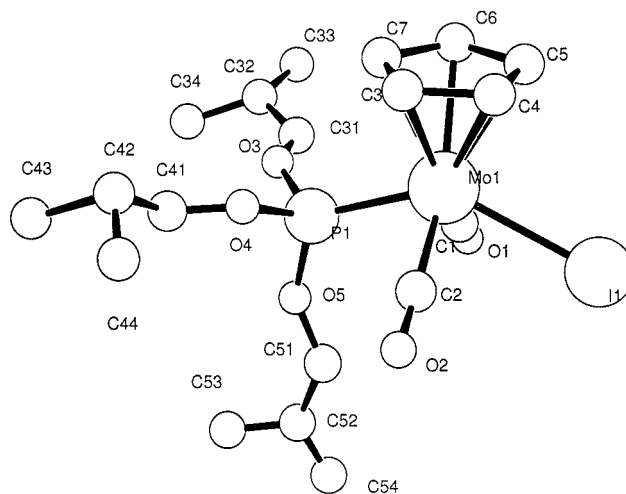


Figure 4. Ball and stick diagram and atomic numbering scheme of $[\text{Mo}(\eta^5\text{-C}_5\text{H}_5)(\text{CO})_2(\text{P}(\text{O}^t\text{Bu})_3)\text{I}]$, **4**. Hydrogen atoms omitted for clarity.

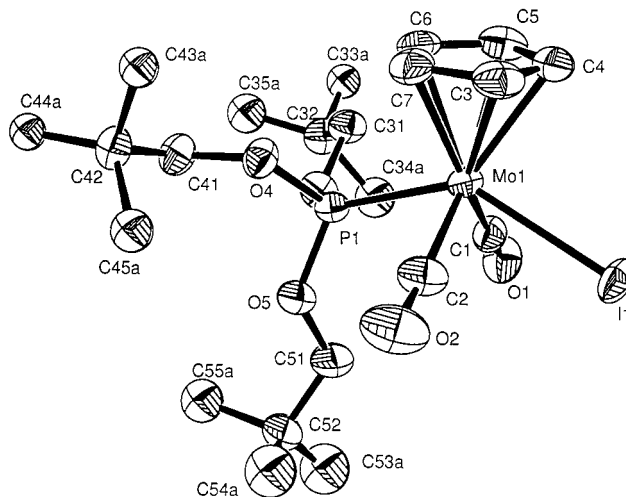


Figure 5. ORTEP diagram and atomic numbering scheme of $[\text{Mo}(\eta^5\text{-C}_5\text{H}_5)(\text{CO})_2(\text{P}(\text{OEt})_3)\text{I}]$, **5**. Hydrogen atoms omitted for clarity. Thermal ellipsoids shown at 30% probability.

greater variation in the phosphite conformation. There is also greater variability in the O–C bond lengths and the P–O–C bond angles than the P–O bond lengths and Mo–P–O bond angles. Beyond the α -carbons, the conformation of the phosphite ligands does not appear to be influenced by the metal–ligand set, and it is at this level that disorder is observed in the ligands. Intermolecular forces will hence play a greater role in establishing possible conformers in this region of space.

Tolman Cone and Solid Angle Measurements from Crystal Structure Data. Tolman cone angles, θ_C , and solid angles, Ω_C , of the phosphite ligands were determined from their conformations in the X-ray crystal structures of complexes **1**–**5**. For consistency with previous work,¹ we have set the Mo–P bond length at 2.28 Å. Since the Mo–P bond lengths were found to be invariant across the series (Table 2), any change in bond length should affect all ligands equally. The multiple ligand conformations in complexes **2** and **5** allowed us to calculate more than one set of steric parameters for these ligands, from which we could estimate relative errors of $\pm 2^\circ$ in θ_C , and $\pm 0.2^\circ$ in Ω_C . Another series of crystal structures for complexes in

Table 2. Selected Bond Lengths (Å) and Angles (deg) for Complexes 1,³⁷ 2, 3, and 5

	1, L = P(OMe) ₃	2, L = P(OEt) ₃	3, L = P(O ⁱ Pr) ₃	5, L = P(O ⁿ Pn) ₃
Mo(1)–P(1)	2.406(9)	2.396(2)	2.400(2)	2.392(1)
Mo(1)–C(1)	2.03(5)	1.991(7)	1.987(8)	1.963(5)
Mo(1)–C(2)	2.01(4)	1.962(8)	1.987(9)	1.963(5)
Mo(1)–I(1)	2.836(4)	2.8628(6)	2.8373(8)	2.85(2)
Mo(1)–cen ^a		2.0024(5)	1.9963(5)	1.9967(7)
P(1)–O(3)	1.60(2)	1.599(5)	1.569(6)	1.578(3)
P(1)–O(4)	1.52(3)	1.579(5)	1.615(7)	1.574(3)
P(1)–O(5)	1.61(3)	1.597(5)	1.615(7)	1.589(3)
O(3)–C(31)	1.53(4)	1.454(8)	1.34(2)	1.435(6)
O(4)–C(41)	1.52(7)	1.443(9)	1.44(1)	1.451(6)
O(5)–C(51)	1.57(5)	1.447(8)	1.41(1)	1.416(7)
C(1)–Mo(1)–C(2)	109(2)	107.5(3)	110.3(3)	106.3(2)
C(1)–Mo(1)–P(1)	78(1)	76.6(2)	77.4(2)	77.8(1)
C(2)–Mo(1)–P(1)	79(1)	79.9(2)	79.7(3)	78.3(2)
P(1)–Mo(1)–I(1)	136(2)	135.22(4)	136.99(2)	137.9(8)
P(1)–O(3)–C(31)	123(2)	122.1(4)	133.7(9)	126.2(3)
P(1)–O(4)–C(41)	117(3)	123.2(6)	128.9(8)	124.8(3)
P(1)–O(5)–C(51)	120(3)	123.3(4)	132.3(6)	123.1(4)
Mo(1)–P(1)–O(3)	122(1)	118.9(2)	119.1(4)	121.3(1)
Mo(1)–P(1)–O(4)	113(1)	112.6(2)	107.8(3)	110.8(1)
Mo(1)–P(1)–O(5)	118(1)	119.5(2)	120.2(4)	118.2(2)
cen ^a –Mo(1)–P(1)–O(5)	–151	–151	–166	–154

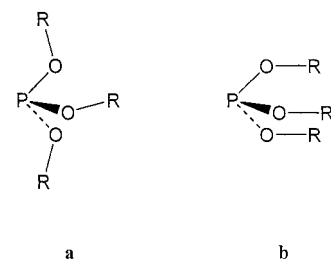
^a cen = cyclopentadienyl ring centroid.**Table 3. Steric and Electronic Parameters for the Phosphite Ligands**

L	χ _i ^a	θ ^b	θ _E ^c	θ _C ^d	θ _{C'} ^e	Ω ^f	Ω _C ^d	Ω _{C'} ^e	E _R ^g
P(OMe) ₃	8.03	107	128	131	127	2.56	2.14	2.32	52
P(OEt) ₃	7.20	109	134	140	134	2.51	2.71	2.63	59
P(O ⁱ Pr) ₃	6.35	130		139	140	3.17	3.17	2.90	74
P(O ⁱ Bu) ₃	7.09 ^h	116 ⁱ		144			2.87		
P(O ⁿ Pn) ₃	7.04 ^h	140 ⁱ		151			3.36		

^a Determined from Ni(CO)₃(L), relative to P(^tBu)₃.¹⁷ ^b Determined from Ni⁰ complexes.¹ ^c Determined from equilibrium studies in [Ti(η⁴-2,4-C₇H₁₁)₂(L)] complexes.^{30,31} ^d Crystallographic cone angle or solid angle, determined from *trans*-[Mo(η⁵-C₅H₅)(CO)₂(L)] (this work). ^e Crystallographic cone angle or solid angle, determined from [W(I)₂(CO)₂(L){Ph₂P(CH₂)₂PPh₂}]³³ (this work). ^f Determined from conformations calculated by molecular mechanics in [Cr(CO)₅(L)].^{4,20} ^g Determined from conformations calculated by molecular mechanics in [Cr(CO)₅(L)].^{2,21} ^h Estimated from regression analysis of PR₃ and P(OR)₃.¹⁷ ⁱ Determined by the Tolman method.¹

which only the phosphite ligand is varied, [W(I)₂(CO)₂(L)(Ph₂P(CH₂)₂PPh₂)] (L = P(OMe)₃, P(OEt)₃, P(OⁱPr)₃) **6–8**,³³ has also recently been reported.⁴² Thus, for comparison, another set of crystallographic cone (θ_C) and solid (Ω_C) angles were determined. Both sets of calculated parameters are listed in Table 3, along with reported literature values for θ and Ω.

Two key points emerge from examination of the crystallographic cone angles, θ_C and θ_{C'}: (i) All θ_C values determined from the crystal structure data are greater than those reported by Tolman, confirming previous observations reported for the phosphite ligands in the “open titanocene” adduct [Ti(η⁴-2,4-C₇H₁₁)₂(L)] (L = P(OMe)₃,³⁰ P(OEt)₃³¹). In all cases, the larger cone angle is a result of a ligand conformation that is different from that used by Tolman. In the crystal structures, two of the alkoxy arms of the ligand are bent back from the third (Figure 6a),^{30,31} while that used by Tolman has

**Figure 6.** Two possible conformations of P(OR)₃. (a) Conformation observed in the crystal structures **1–3** and **5**. (b) Conformation used by Tolman¹ to determine cone angles.

C_{3v} symmetry with all three alkoxy arms pointing away from the metal (Figure 6b). (ii) In contrast with the values of the cone angles determined from the tungsten structures **6–8**, those determined from the molybdenum structures **1–5** do not show the intuitively expected trend. In particular, the measurements from these structures show the crystallographic cone angle of P(OEt)₃ to be about the same as that of P(OⁱPr)₃. This anomalous result can be explained by consideration of the *angular profiles*^{25,27,43–48} of these two ligands (Figure 7) and consideration of the fact that the cone angle for a conformationally nonsymmetric ligand is determined as the average of the semi-cone angles of the three groups attached to the phosphorus atom.¹ The angular profiles qualitatively reveal that the semi-cone angles are approximately the same in both ligands, leading to similar cone angles. However, the total area enclosed by the profile for the P(OⁱPr)₃ ligand is larger, which is reflected in its solid angle value (see below). Likewise, the larger cone angle, but smaller solid angle, of

(43) Alyea, E. C.; Dias, S. A.; Ferguson, G.; Restivo, R. J. *Inorg. Chem.* **1977**, *16*, 2329–2334.

(44) Smith, J. D.; Oliver, J. D. *Inorg. Chem.* **1978**, *17*, 2585–2589.

(45) Farrar, D. H.; Payne, N. C. *Inorg. Chem.* **1981**, *20*, 821–828.

(46) Alyea, E. C.; Ferguson, G.; Somogyvari, A. *Inorg. Chem.* **1982**, *21*, 1369–1371.

(47) Alyea, E. C.; Dias, S. A.; Ferguson, G.; Siew, P. Y. *Can. J. Chem.* **1983**, *61*, 257–262.

(48) Mullica, D. F.; Gipson, S. L.; Sappenfield, E. L.; Lin, C. C.; Leschnitzer, D. H. *Inorg. Chim. Acta* **1990**, *177*, 89–96.

(42) This series of seven coordinate complexes might be expected to be sterically crowded, which would be manifested in smaller W–P–O angles. However, these angles are in the same range as for our molybdenum complexes. For example, in the complex [W(I)₂(CO)₂(L)(Ph₂P(CH₂)₂PPh₂)] **4**, the W–P–O angles show the same trend as for the molybdenum complexes, with one smaller angle at 110° and two larger angles at 119° and 125°.

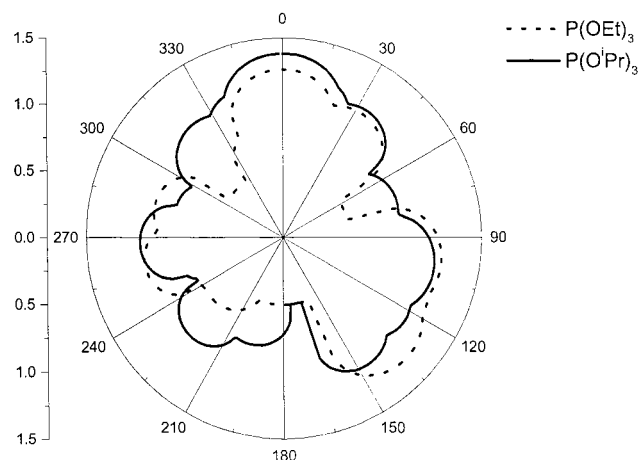


Figure 7. Angular profiles of the ligands P(OEt)₃ and P(OPr)₃ taken from the crystal structures of **2** and **3**.

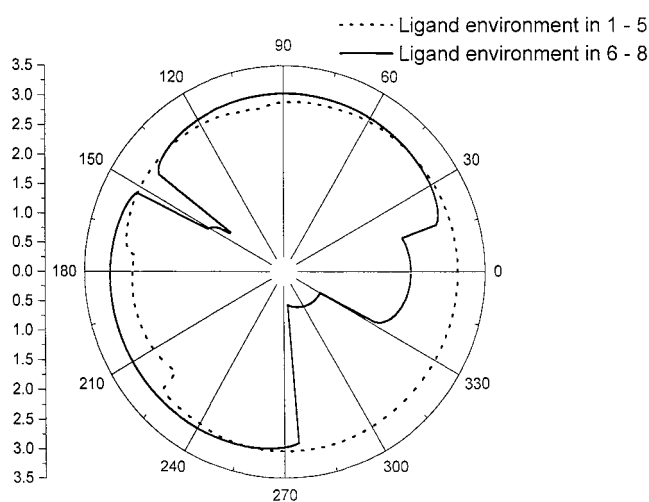


Figure 8. Angular profiles of the phosphite ligand environments, excluding the phosphite ligand, in [Mo(η^5 -C₅H₅)(CO)₂(L)I] and [W(I)₂(CO)₂(L){Ph₂P(CH₂)₂PPh₂}]. (a) Ligand environment of complexes **1–5**. (b) Ligand environment of complexes **6–8**.

P(O^{*i*}Bu)₃ as compared to P(O^{*i*}Pr)₃ can be similarly rationalized. In the case of the tungsten complexes **7** and **8**, there is a greater difference in the semi-cone angles of the P(O^{*i*}Pr)₃ and P(O^{*i*}Bu)₃ ligands, leading to cone angles that are the expected relative sizes. Angular profiles of the remaining ligands in the complex, i.e., with the exception of the phosphite ligand, can also help rationalize the relative effect of the ligand environment on the phosphite cone angle (Figure 8). Further, cone angle values of the metal fragments can be calculated to obtain a semiquantitative idea of the sizes of the respective ligand environment. Both the angular profiles and the cone angle data clearly show that the ligand environment created by the [Mo(η^5 -C₅H₅)(CO)₂I] (209°) fragment in **1–5** is less sterically demanding than that created by [W(I)₂(CO)₂(Ph₂P(CH₂)₂PPh₂)] (248°) in **6–8**. Thus, for conformationally flexible ligands such as the phosphites, the size of the ligand should be influenced by the ligand environment, as is observed.

The calculated solid angles show trends similar to that of the cone angles. It is clear, however, that the solid angles are more sensitive to the conformation of the ligand. This is reflected in both the larger relative

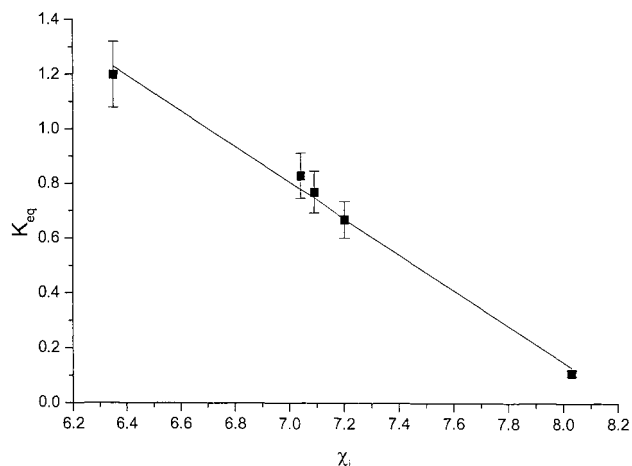


Figure 9. Electronic profile of K_{eq} for complexes **1–5**.

error in the solid angle data (ca. 5% for the Ω_C , compared to ca. 1% for θ_C) and the greater variation in the solid angles between the two sets of phosphite structural data.

Correlation of Structurally Determined θ or Ω with *cis–trans* Isomer Ratios. The solution equilibrium *cis–trans* isomer ratios (K_{eq}) of **1–5** are presented in Table 1. These isomer ratios have been proposed to depend on both steric and electronic factors.⁴⁹

Regression analysis of K_{eq} with the electronic parameter, χ_1 (electronic profile, Figure 9), gives an excellent correlation ($R^2 = 0.993$, $mse = 0.002$), which suggests that the equilibrium isomer ratio is predominantly influenced by electronic factors. This result suggests that better electron-donating ligands lead to a larger *cis* to *trans* ratio.

Since the isomer ratio appears to correlate strongly with electronic effects, there should be a minor, if any, dependence, on steric factors. Including either θ_C or Ω_C in the regression analysis resulted in a marginal improvement in the quality of the regression (Table 3). The results obtained using the crystallographic cone angle data are actually better than those obtained using the crystallographic solid angle data; the best fit to the data is shown in eq 2. Regression analysis using the original Tolman cone angles lowers the quality of the correlation slightly (Table 3).

$$K_{eq} = (4.4 \pm 0.1) - (0.623 \pm 0.06)\chi_1 + (0.0054 \pm 0.00005)\theta_C \quad (2)$$

Thus, increasing the size of the ligand appears to slightly favor formation of the *cis* over the *trans* isomer, but overall there is only a small dependence on steric effects. A steric profile using the crystallographic cone angle θ_C was also plotted (Figure 10), and the scatter of the data makes it impossible to determine the presence or lack of a steric threshold.^{7,10,50}

(49) Faller, J. W.; Anderson, A. S.; Chen, C.-C. *J. Organomet. Chem.* **1969**, *17*, P7–P7.

(50) As suggested to us by a referee, we have also examined the isomerization behavior of the complex containing the ligand P(OCH₂)₃-Cet. An advantage of using this ligand is that there is no controversy regarding its Tolman cone angle (101°). Unfortunately, we did not observe any *trans*→*cis* isomerization for the complex [Mo(η^5 -C₅H₅)(P(OCH₂)₃Cet)(CO)₂I], which is not totally surprising, as it has the greatest electron-withdrawing character of the ligands studied ($\chi_1 = 10.4$). It is thus clear that electronic effects dominate.

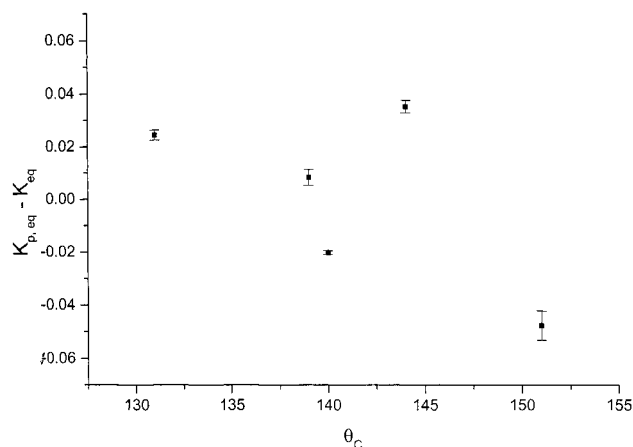


Figure 10. Crystallographic cone angle (θ_c) steric profile of K_{eq} for complexes **1–5**. $K_{eq,p}$ is the value of K_{eq} predicted on the basis of electronic effects alone; thus $K_{eq} - K_{eq,p}$ gives the difference between the equilibrium constant and that predicted on the basis of electronic effects alone.

The variability of cone angle values has serious implications for the quantitative analyses of physical and chemical properties in terms of steric effects, such as QALE.^{7,10,11} An inherent weakness of the QALE approach used to date is that no variation in the steric parameters has been considered; parameters used have been considered to be absolute. Our analysis shows that electronic factors determine K_{eq} ⁵¹ for the molybdenum complexes **1–5**. Thus the system is a poor one for testing steric parameters. Other systems may be expected to show a greater effect.

Conclusion

Analysis of the crystal structures of the complexes *trans*-[Mo(η^5 -C₅H₅)(CO)₂(L)I] (L = P(OMe)₃, P(OEt)₃, P(OⁱPr)₃, P(OⁱBu)₃, and P(OⁿPn)₃) showed the coordination environment available to the phosphite ligand to be similar in all cases. The crystallographic cone, θ_c , and solid, Ω_c , angles of the ligands, L, were determined from the crystal structures of these ligands and compared with literature and other calculated data. Anomalous results in the values of the relevant steric parameters could be rationalized by examining the ligand conformation, particularly by the use of angular profiles. The cone angles determined from crystal structures showed some variation in their values, but *all* were found to be larger than those reported by Tolman. This variability in steric values, which will be further addressed in a subsequent publication, has serious implications for methods that use ligand parameters quantitatively, such as QALE, and could lead to revised conclusions in such analyses.

Experimental Section

General Procedures. All reactions were carried out under a nitrogen atmosphere using standard Schlenk techniques. Solvents were dried by conventional methods, distilled under nitrogen, and used immediately. The compounds [Mo(η^5 -C₅H₅)(CO)₃]₂, P(OEt)₃, P(OⁱPr)₃, and P(OⁱBu)₃ were obtained from Strem Chemicals and used as received; [Mo(η^5 -C₅H₅)(CO)₃I] was prepared by treating [Mo(η^5 -C₅H₅)(CO)₃]₂ with elemental

Table 4. Results of Regression Analyses of K_{eq} for [Mo(η^5 -C₅H₅)(CO)₂(L)I]

	crystallographic cone angle, θ_c	crystallographic solid angle, Ω_c	Tolman cone angle, θ
R^2	0.9999	0.9988	0.9955
mse	3.17×10^{-5}	3.68×10^{-4}	1.38×10^{-3}

iodine.⁵² P(OⁿPn)₃ was purified by vacuum distillation and Me₃NO by the thermal dehydration of Me₃NO·2H₂O in vacuo. Infrared spectra were recorded on a Jasco FT/IR 5000 spectrometer in KBr cells and NMR spectra on a Bruker AC-200 spectrometer operating at 200 MHz. Differential scanning calorimetry was performed on 5–15 mg samples under flowing nitrogen at a constant heating rate of 10°/min on a Du Pont 910 DSC instrument. Melting points were obtained from the DSC thermograms. Microanalyses were carried out at the CSIR, Pretoria, South Africa.

Preparation of [Mo(η^5 -C₅H₅)(CO)₂(L)I], L = P(OMe)₃,³⁵ P(OEt)₃, P(OⁱPr)₃, P(OⁱBu)₃, and P(OⁿPn)₃, **1–5.** A solution of [Mo(η^5 -C₅H₅)(CO)₃I] (250 mg, 0.510 mmol) and the ligand L (2.4 mmol) in dichloromethane (20 mL) was prepared while purging the solution with N₂. To this solution was added Me₃NO (100 mg, 1.33 mmol), which caused immediate effervescence. The progress of the reaction was monitored by the disappearance of the 2044 cm⁻¹ peak in the IR spectrum. On completion, the dark red color of the solution had faded to orange. The solvent was removed by rotary evaporation, and the residue was extracted with CHCl₃ and purified by column chromatography (CoCl₂·6H₂O, alumina I, 50% CHCl₃/hexane). Crystals were grown from CH₂Cl₂/hexane solutions at -18 °C. All complexes were found to crystallize exclusively as the *trans* isomer and occurred as red, air-stable complexes, except for L = P(OⁱBu)₃, which decomposed to a black solid at room temperature.

***trans*-[Mo(η^5 -C₅H₅)(CO)₂(P(OMe)₃)I] (**1a**):** ¹H NMR (C₆D₆) δ 4.84 (d, J_{PH} = 1.6 Hz, 5H, C₅H₅); 3.34 (d, J_{PH} = 11.8, 3H, OMe); IR (C₆D₆) ν_{CO} = 1975, 1901 cm⁻¹.

***cis*-[Mo(η^5 -C₅H₅)(CO)₂(P(OMe)₃)I] (**1b**):** ¹H NMR (C₆D₆) δ 5.07 (s, 5H, C₅H₅); 3.16 (t, J_{PH} = 11.6, 3H, OMe).

***trans*-[Mo(η^5 -C₅H₅)(CO)₂(P(OEt)₃)I] (**2a**):** Mp 59 °C; ¹H NMR (C₆D₆) δ 4.90 (d, J_{PH} = 1.9 Hz, 5H, C₅H₅); 3.71 (dq, J_{PH} = 7.1 Hz, J_{HH} = 7.0, 2H, OCH₂); 1.07 (t, J_{HH} = 7.0, 3H, CH₃); IR (C₆D₆) 1974, 1896 cm⁻¹. Anal. Calcd for C₁₃H₂₀IO₅MoP (510.10): C, 30.61; H, 3.95. Found: C, 30.30; H, 3.82.

***cis*-[Mo(η^5 -C₅H₅)(CO)₂(P(OEt)₃)I] (**2b**):** ¹H NMR (C₆D₆) δ 4.88 (s, 5H, C₅H₅); 3.93 (m, J_{AB} = 4.0 Hz, J_{PH} = 7.1 Hz, J_{HH} = 7.0 Hz, 1H, OCH_A); 3.89 (m, J_{AB} = 4.0 Hz, J_{PH} = 7.1 Hz, J_{HH} = 7.0 Hz, 1H, OCH_B); 0.90 (t, J_{HH} = 7.0, 3H, CH₃).

***trans*-[Mo(η^5 -C₅H₅)(CO)₂(P(OⁱPr)₃)I] (**3a**):** Mp 160 °C; ¹H NMR (C₆D₆) δ 4.95 (d, J_{PH} = 1.8 Hz, 5H, C₅H₅); 4.50 (m, J_{PH} = 9.4 Hz, J_{HH} = 6.1 Hz, 1H, OCH); 1.04 (d, J_{HH} = 6.1, 6H, CH₃). IR (C₆D₆) = 1971, 1893 cm⁻¹. Anal. Calcd for C₁₆H₂₆IO₅MoP (552.18): C, 34.80; H, 4.75. Found: C, 34.73; H, 4.69.

***cis*-[Mo(η^5 -C₅H₅)(CO)₂(P(OⁱPr)₃)I] (**3b**):** ¹H NMR (C₆D₆) δ 4.88 (s, 5H, C₅H₅); 4.70 (m, J_{PH} = 9.2 Hz, J_{HH} = 6.1 Hz, 1H, OCH); 1.18 (d, J_{HH} = 6.1, 6H, CH₃).

***trans*-[Mo(η^5 -C₅H₅)(CO)₂(P(OⁱBu)₃)I] (**4a**):** Mp 104 °C (dec); ¹H NMR (C₆D₆) δ 4.97 (d, J_{PH} = 1.8 Hz, 5H, C₅H₅); 3.68 (dd, J_{PH} = 6.0 Hz, J_{HH} = 6.7, 2H, OCH₂); 1.71 (d, J_{HH} = 6.7, 1H, CH); 0.80 (d, J_{HH} = 6, 6H, CH₃); IR (C₆D₆) 1971, 1896 cm⁻¹. Anal. Calcd for C₁₉H₃₂IO₅MoP (594.26): C, 38.40; H, 5.43. Found: C, 38.09; H, 5.34.

***cis*-[Mo(η^5 -C₅H₅)(CO)₂(P(OⁱBu)₃)I] (**4b**):** ¹H NMR (C₆D₆) δ 4.93 (s, 5H, C₅H₅); 3.84 (m, J_{AB} = 3.5 Hz, J_{PH} = 6.0 Hz, J_{HH} = 6.7, 1H, OCH_A); 3.83 (m, J_{AB} = 3.5 Hz, J_{PH} = 6.0 Hz, J_{HH} = 6.7, 1H, OCH_B); 1.87 (1H, CH); 0.89 (d, J_{HH} = 6.7, 3H, CH₃); 0.88 (d, J_{HH} = 6.7, 3H, CH₃).

(51) Similar results were obtained for the analysis using log(K_{eq}); however, the quality of fit was generally lower.

(52) Davis, R. *Molybdenum Compounds with η^2 - η^6 Carbon Ligands*; Wilkinson, G., Stone, F. G. A., Abel, E. W., Eds.; Pergamon Press: Oxford, 1982; Vol. 3, pp 1187–1185.

Table 5. Crystal Data and Details of Structure Refinement for Complexes 2, 3, and 5

	2, L = P(OEt)₃	3, L = P(OⁱPr)₃	5, L = P(OⁿPn)₃
empirical formula	C ₁₉ H ₃₂ IO ₅ MoP	C ₁₆ H ₂₆ IO ₅ MoP	C ₂₂ H ₃₈ IO ₅ MoP
fw	594.26	552.18	636.33
temperature/K	296(2)	293(2)	293(2)
wavelength/Å	0.71073	0.71069	0.71069
cryst syst, space group	triclinic, <i>P</i> $\bar{1}$	monoclinic, <i>Cc</i>	triclinic, <i>P</i> $\bar{1}$
unit cell dimens	<i>a</i> = 17.3351(12) Å, α = 90° <i>b</i> = 17.3218(12) Å, β = 91.834(2)° <i>c</i> = 8.7305(6) Å, γ = 90°	<i>a</i> = 10.1591(19) Å, α = 90° <i>b</i> = 13.9064(13) Å, β = 97.881(11)° <i>c</i> = 15.6572(11) Å, γ = 90°	<i>a</i> = 8.902(3) Å, α = 82.089(13)° <i>b</i> = 10.4504(18) Å, β = 78.99(2)° <i>c</i> = 17.026(3) Å, γ = 66.942(18)°
volume/Å ³	2620.2(3)	2191.1(5)	1427.1(5)
<i>Z</i> , ρ_{calc} /Mg m ⁻³	4, 1.506	4, 1.674	2, 1.481
abs coeff/mm ⁻¹	1.762	2.100	1.623
<i>F</i> (000)	1184	1088	640
cryst size/mm	1.04 × 0.28 × 0.10	0.43 × 0.32 × 0.17	0.58 × 0.24 × 0.13
θ range for data collection/deg	1.66–28.31	2.50–34.95	2.12–29.99
limiting indices	–21 ≤ <i>h</i> ≤ 22, –18 ≤ <i>k</i> ≤ 22, –11 ≤ <i>l</i> ≤ 11	–16 ≤ <i>h</i> ≤ 16, –1 ≤ <i>k</i> ≤ 22, –1 ≤ <i>l</i> ≤ 25	–12 ≤ <i>h</i> ≤ 12, –14 ≤ <i>k</i> ≤ 14, 0 ≤ <i>l</i> ≤ 23
reflins collected/unique	14378/5781 [<i>R</i> (int) = 0.0423]	5553/5211 [<i>R</i> (int) = 0.0131]	8570/8309 [<i>R</i> (int) = 0.0397]
completeness to θ = 29.99	88.5%	99.8%	99.9%
max. and min. transmsn	0.8435 and 0.2616	0.7166 and 0.4654	0.8167 and 0.4529
refinement method	full-matrix least-squares on <i>F</i> ²	full-matrix least-squares on <i>F</i> ²	full-matrix least-squares on <i>F</i> ²
no. of data/restraints/params	5781/2/271	5211/2/202	8309/0/363
goodness-of-fit on <i>F</i> ²	0.998	1.193	0.918
final <i>R</i> indices [<i>I</i> > 2 σ (<i>I</i>)]	<i>R</i> 1 = 0.0782, <i>wR</i> 2 = 0.1740	<i>R</i> 1 = 0.0615, <i>wR</i> 2 = 0.1174	<i>R</i> 1 = 0.0510, <i>wR</i> 2 = 0.1432
<i>R</i> indices (all data) ^a	<i>R</i> 1 = 0.1811, <i>wR</i> 2 = 0.2200	<i>R</i> 1 = 0.0619, <i>wR</i> 2 = 0.1176	<i>R</i> 1 = 0.0717, <i>wR</i> 2 = 0.1606
largest diff peak and hole/e Å ⁻³	0.790 and –0.523	0.697 and –0.683	0.973 and –0.398

$$^a R1 = \sum(|F_o| - |F_c|)/\sum|F_o|, R2 = \sum w_2(|F_o|^2 - |F_c|^2)^2 \text{ where } w_2 = 1/(\sum|F_o|^2 + (0.0766 \times ((\max(F_o^2, 0) + 2 \times |F_c|^2)/3))).$$

trans-[Mo(η^5 -C₅H₅)(CO)₂(P(OⁿPn)₃)I] (5a): Mp 190 °C (dec); ¹H NMR (C₆D₆) δ 5.00 (d, *J*_{PH} = 1.9 Hz, 5H, C₅H₅); 3.65 (d, *J*_{PH} = 4.9 Hz, 2H, OCH₂); 0.84 (s, 3H, CH₃). IR (C₆D₆) = 1974, 1893 cm⁻¹. Anal. Calcd for C₂₂H₃₈IO₅MoP (636.34): C, 41.52; H, 5.70. Found: C, 41.52; H, 5.95.

cis-[Mo(η^5 -C₅H₅)(CO)₂(P(OⁿPn)₃)I] (5b): ¹H NMR (C₆D₆) δ 4.94 (s, 5H, C₅H₅); 3.83 (m, *J*_{AB} = 4.2 Hz, *J*_{PH} = 4.9 Hz, 1H, OCH_A); 3.80 (m, *J*_{AB} = 4.2 Hz, *J*_{PH} = 4.9 Hz, OCH_B); 0.84 (s, 3H, CH₃).

Single-Crystal X-ray Crystallography of [(η^5 -C₅H₅)Mo(CO)₂(L)I], L = P(OEt)₃, P(OⁱPr)₃, and P(OⁿPn)₃. Dark red crystals of [Mo(η^5 -C₅H₅)(CO)₂(L)I], L = P(OEt)₃, P(OⁱPr)₃, and P(OⁿPn)₃, **2–5**, were obtained by crystallization from CH₂Cl₂/hexanes mixtures at –18 °C. For complexes **3** and **5**, diffraction quality crystals were selected with oscillation and Weissenburg techniques, using Cu K α radiation. The approximate cell constants and the apparent space groups were determined from the resultant photographs. Unit cell and intensity data were measured at room temperature on an Enraf-Nonius CAD4 single-crystal diffractometer using graphite-monochromated Mo K α radiation. Accurate cell constants were obtained by least-squares refinement of 25 high-order reflections. Intensities were measured in ω –2 θ scan mode at a maximum scan speed of 5.49 (**3**) or 4.12 (**5**) deg/min and a minimum scan time of 90 s per reflection. Data reduction consisted of correction for background and Lorentz–polarization factors using PROFIT.^{53,54} Analytical absorption corrections were made using the XTAL 3.2⁵⁵ suite of programs.

To monitor crystal and instrument stability and to enable crystal decay corrections, three reference intensities were measured every 120 (**3**) or 200 (**5**) min during the data collection. Crystal decay was found to be negligible.

The final data set after internal scaling consisted of 5553 (**3**) and 8570 (**5**) reflections to 0.90 Å resolution. Coverage of all data is 99.8% (**3**) or 99.9% (**5**) complete to at least 28° (**3**)

or 30° in θ . Details of the data collection and refinement are listed in Table 4.

For complex **2**, the X-ray data set was collected on the novel 1K SMART Siemens CCD area detector system using Mo radiation. X-rays were generated using a regular sealed tube and an X-ray generator operating at 50 kV and 30 mA. The 9 cm wide CCD area detector was mounted 4.5 cm from the crystal, and the data set collected at room temperature. A graphite monochromator followed by a 0.5 mm collimator was used. The selected crystal was mounted on a thin glass fiber.

To obtain an initial set of cell parameters and an orientation matrix for data collection, 88 reflections from three sets of 15 frames each were collected covering three perpendicular sectors of space.

The data collection nominally covered over a full sphere/hemisphere of reciprocal space, by a combination of three sets of exposures, 1271 frames. Each set had a different φ angle for the crystal and each exposure covered 0.3° in ω , with 5 s exposure time per frame.

To monitor crystal and instrument stability and to enable crystal decay corrections, the first 50 frames of the first set were measured again at the end of the data collection. Crystal decay was found to be negligible after analyzing the duplicate reflections.

The final data set after internal scaling consisted of 14 378 reflections to 0.90 Å resolution. Coverage of all data is 98.68% complete to at least 25° in θ . The data collection took about 4 h. Details of the data collection and refinement are listed in Table 4.

The determination of the unit cell parameters, crystal orientation, and data collection were performed with SMART.⁵⁶ The crystallographic raw data frames were integrated, and all reflections were extracted, reduced, and *Lp*-corrected using the program SAINT.⁵⁷ The cell refinement using all data was

(53) Streltsov, V. A.; Zavodnik, V. E. *Sov. Phys.-Cryst.* **1989**, *34*.

(54) Streltsov, V. A.; Zavodnik, V. E. *Soc. Phys.-Cryst.* **1990**, *35*.

(55) Davenport, G. M.; Spadaccini, N.; Stewart, J. *ABSORB*; Hall, S. R., Flack, H. D., Stewart, J. M., Eds.; Lamb: Perth, 1992.

(56) *SMART Reference Manual*; Siemens Analytical X-ray Instruments Inc.: Madison, WI, 1997–1998.

(57) *ASTRO and SAINT. Data Collection and Processing Software for the SMART System*; Siemens Analytical X-ray Instruments Inc.: Madison, WI, 1997–1998.

performed by SAINT.⁵⁷ The program SHELXTL ver 5.1⁵⁸ was used for structure solution, refinement, molecular graphics, and publication preparation of all complexes.

Cis–trans Isomerization Studies of $[(\eta^5\text{-C}_5\text{H}_5)\text{Mo}(\text{CO})_2(\text{L})\text{I}]$, $\text{L} = \text{P}(\text{OEt})_3$, $\text{P}(\text{O}^i\text{Pr})_3$, $\text{P}(\text{O}^i\text{Bu})_3$, and $\text{P}(\text{O}^n\text{Pn})_3$ The equilibrium ratio of the *cis* and *trans* isomers was achieved by heating a solution of the relevant complex in C_6D_6 at 60–70 °C in an NMR tube until equilibrium was established, typically within 8 h. The position of the equilibrium was found to have no dependence on temperature within this range. The equilibrium ratios are listed in Table 1. The possibility of isomerization occurring in the solid state was probed by the use of DSC. However, only the exotherm corresponding to melting of the solid was observed.

Steric Parameter Calculations. Cone, θ , and solid, Ω , angles were calculated according to literature procedures^{1,4,19,20,59} using the program Steric⁶⁰ on a Pentium 450 PC operating on Red Hat Linux. The ligand conformations for $\text{P}(\text{OEt})_3$, $\text{P}(\text{O}^i\text{Pr})_3$, $\text{P}(\text{O}^i\text{Bu})_3$, and $\text{P}(\text{O}^n\text{Pn})_3$ were obtained from the crystal structures of **2–5**, while that of $\text{P}(\text{OMe})_3$ was obtained

from the crystal structure of *trans*- $[\text{Mo}(\eta^5\text{-C}_5\text{H}_5)(\text{CO})_2(\text{P}(\text{OMe})_3)\text{I}]$.³⁷ Hydrogen atoms, as placed in the crystallographic determination, were fixed at average C–H bond distances obtained from neutron diffraction data.⁶¹ In accordance with previous work,^{1,19} Mo–P bond lengths were fixed at 2.28 Å. For Tolman cone angle calculations, the CPK van der Waals radii set was used, while for solid angle calculations, the Bondi data set⁶² was used, also in accordance with previous work.^{1,4,19,20}

Acknowledgment. We would like to acknowledge the FRD, THRIP, and the University of the Witwatersrand for financial support.

Supporting Information Available: A listing of the atomic coordinates, bond lengths, bond angles, and torsion angles for the crystal structures of **2**, **3**, and **5** is available. Angular profiles of the phosphite ligands in all complexes and steric profiles for the solid angle and Tolman cone angle are also included. This material is available free of charge via the Internet at <http://pubs.acs.org>.

OM000347A

(58) SHELXTLplus Version 5.1 (Windows NT version)–Structure Determination Package; Siemens Analytical X-ray Instruments Inc.: Madison, WI, 1998.

(59) Taverner, B. C. *J. Comput. Chem.* **1996**, *17*, 1612–1623.

(60) Taverner, B. C. *Steric*, 1.12B; 1997. Available on the Internet at <http://www.gh.wits.ac.za>.

(61) Allen, F. H.; Kennard, O.; Watson, D. G.; Brammer, L.; Orpen, A. G.; Taylor, R. *J. Chem. Soc., Perkin Trans. 2* **1987**, S1–S19.

(62) Bondi, A. *J. Phys. Chem.* **1964**, *68*, 441–451.